Design and characterization of new 90 GHz detectors for the Cosmology Large Angular Scale Surveyor (CLASS)

Carolina Núñez[1], John W. Appel[1], Sarah Marie Bruno[1], Rahul Datta[1], & The CLASS Collaboration[1-15]

[1]Johns Hopkins University, [2]University Of California, Berkeley, [3]Goddard Space Flight Center, [4]Harvard & Smithsonian, [5]Los Alamos National Laboratory, [6]Massachusetts Institute of Technology, [7]National Institute of Standards and Technology, [8]University of Oslo, [9]Pontificia Universidad Católica de Chile, [10]University of Chicago, [11]Universidad de Concepción, [12]Universidad Católica de la Santísima Concepción, [13]Universidad de Chile, [14]University of Pennsylvania, [15]Villanova University

INTRODUCTION

Fig. 1: The CLASS telescopes, observing the CMB, from the Parque Astronómico Atacama.

The Cosmology Large Angular Scale Surveyor (CLASS) is a polarization-sensitive telescope array located at an altitude of 5,200 m in the Chilean Atacama Desert. CLASS is designed to measure "E-mode" (even parity) and "B-mode" (odd parity) polarization patterns in the Cosmic Microwave Background (CMB) over large angular scales. CLASS seeks to improve our understanding of inflation, reionization, and dark matter [5, 6].

CLASS observes across four frequency bands via its three currently-fielded telescopes: 40 GHz (Q), 90 GHz (W1), 150/220 GHz (G). We discuss the updated design and in-lab characterization of improved detectors, which will lead to upgraded detectors in W1 in 2022.

FOCAL PLANE DESIGN

Fig. 2: CLASS 90 GHz wafer (left) with detector pixel (top right) and updated Transition Edge-Sensor (TES) (bottom right) architecture. For a full description of the 90 GHz wafer design, see [2, 4, 9]. The three-layer wafers are comprised of: a silicon photonic choke wafer, a monocrystalline silicon detector wafer, and a silicon backshort assembly. Each of the 37 detector pixels consists of a symmetric planar ortho-mode transducer (OMT), which reads out two orthogonal linear polarizations (H/V) over microstrip transmission lines to MoAu bilayer TES bolometers. Bandpasses are defined via on-chip filters. The updated TES architecture includes an improved absorber with a resistive meander, as well as metal connection between the the TES and the Pd.

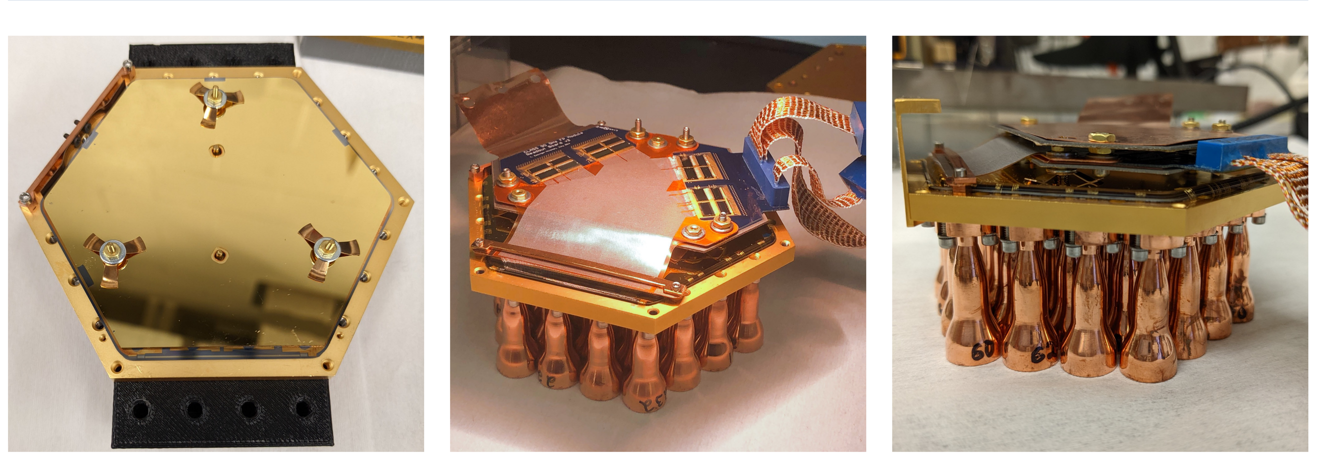

Fig. 3: Each wafer is assembled into a module to facilitate assembly and testing. Smooth-walled feedhorns couple to the TES bolometers. The wafer is mounted and aligned on a Au-plated CE7 baseplate. Au bonds provide heat-sinking from the wafer to the baseplate and Al bonding connects the detector wafer to the readout circuit (RC). The RC consists of a PCB, shunt and MUX chips, an Al flex circuit, and aluminum bonds. The RC is sandwiched between two Nb sheets and heat-sunk with a Cu layer. For a full description of the assembly stack, see [3].

DETECTOR CHARACTERIZATION

CLASS detectors are mounted onto the 100 mK stage of a pulse tube pre-cooled dilution refrigerator [8] via a Au-plated web. The cryostat reaches an operational bath temperature (T_{bath}) of ~50 mK. Four new CLASS 90 GHz wafers were tested in the cryostat at JHU. Dark testing for estimation of electrothermal parameters and noise equivalent power (NEP) is conducted with all stages of the cryostat closed with metal plates. For bandpass measurements, the 4/60 K stages are necked-down with small aperture plates. An ultra-high-molecular-weight polyethylene vacuum window lets in light, while extruded polystyrene foam filters reject out-of-band IR radiation.

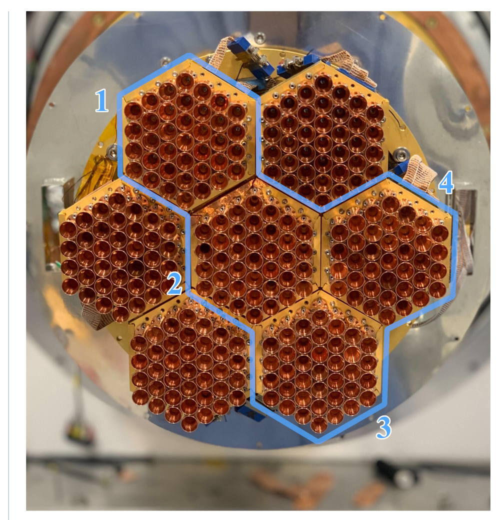

Fig. 4: Four new CLASS 90 GHz modules (outlined in blue) situated in the BlueFors cryostat of the W1 receiver.

I. ELECTROTHERMAL PARAMETERS

I-V curves are used to determine the thermal parameters of the TES bolometers. At each T_{bath}, the voltage bias is ramped down in steps, driving the TES from normal to superconducting. TES current (I_{TES}) and voltage (V_{TES}) are calculated following [1].

Fig. 5: Example I-V curves for one detector. The inverse slope of the normal branch of the I-V yields the normal resistance (R_N) of the TES. The saturation power (P_{sat}), given by $I_{TES} \times V_{TES}$, is defined at 70% R_N. P_{sat} is the amount of power required to raise the TES to its superconducting critical temperature (T_c). T_c and κ are determined assuming $n = 4$ (ballistic phonon limit) [1, 3, 7].

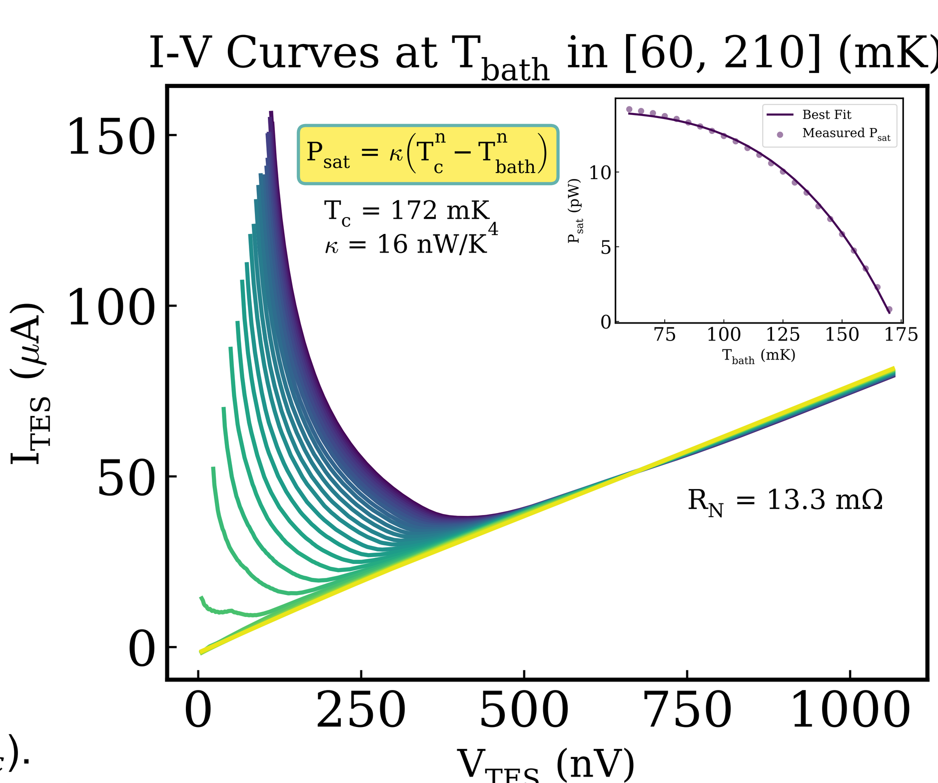

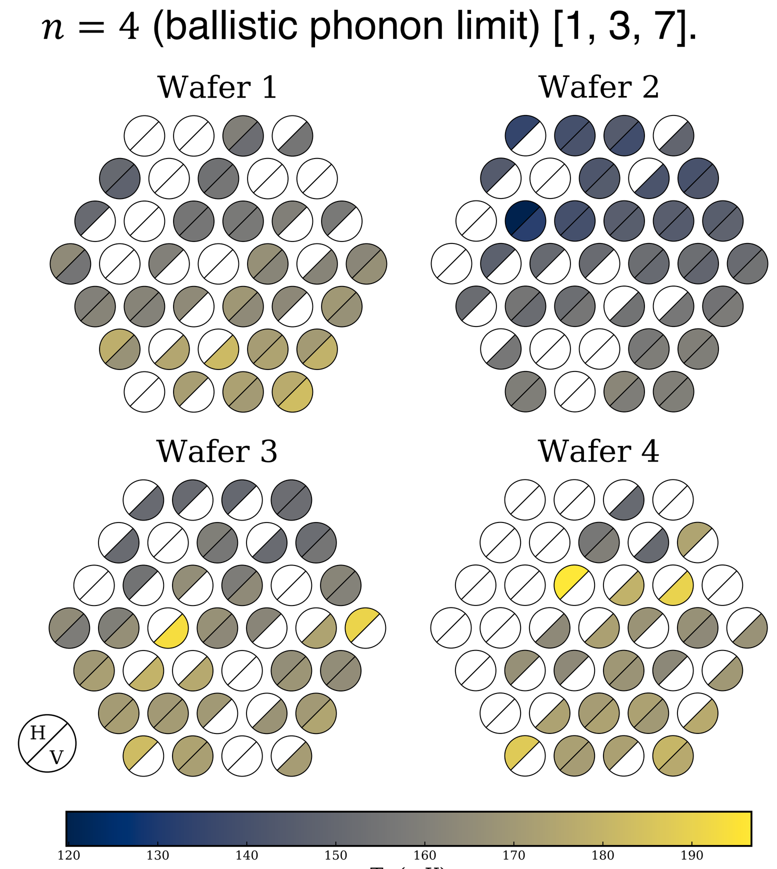

Fig. 6: Measured values of T_c at each detector pixel. T_c values shown are for 175 bolometers that produced good I-V measurements during testing.

Table 1: Median (standard deviation) values for each wafer of key thermal parameters derived from I-V curves. The thermal conductance G is given by $G = n\kappa T_c^{n-1}$. For each wafer (1-4) we report values for approximately 45, 51, 47, and 32 bolometers, respectively.

	Wafer 1	Wafer 2	Wafer 3	Wafer 4
$G(T_c)$ (pW/K)	270. (63)	229 (30.)	257 (53)	304 (56)
κ (nW/K^4)	16 (3.0)	17 (1.0)	14 (3.0)	15 (0.86)
$P_{sat}(50\ mK)$ (pW)	11 (2.9)	8.4 (1.5)	11 (2.6)	13 (3.1)
R_N (mΩ)	12.7 (0.46)	11.0 (0.52)	10.3 (0.35)	10.7 (0.33)
T_c (mK)	163 (8.5)	151 (8.4)	165 (10.)	171 (9.7)

II. BANDPASSES

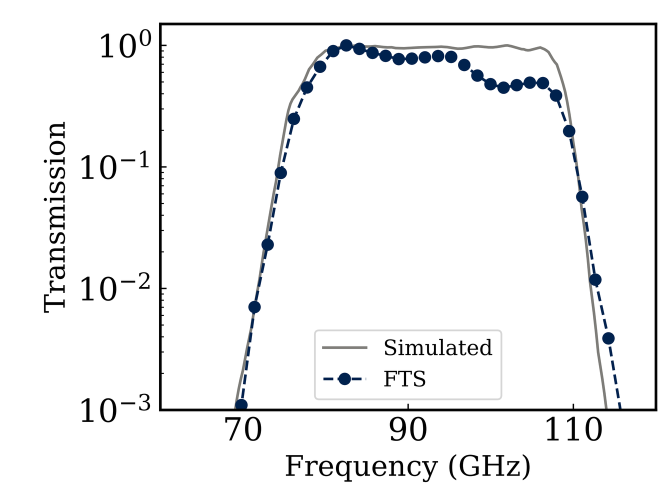

Fig. 7: Average measured and simulated spectral response, normalized to unity. The reported bandpasses were measured using a Fourier Transform Spectrometer at JHU. The band edges are in agreement with the simulations. The measured response plotted is the inverse variance-weighted average of 93 bolometers across three wafers. The discrepancies observed in-band between measured and simulated responses are likely due to optical effects related to the test setup that are not included in the simulation.

III. NOISE EQUIVALENT POWER

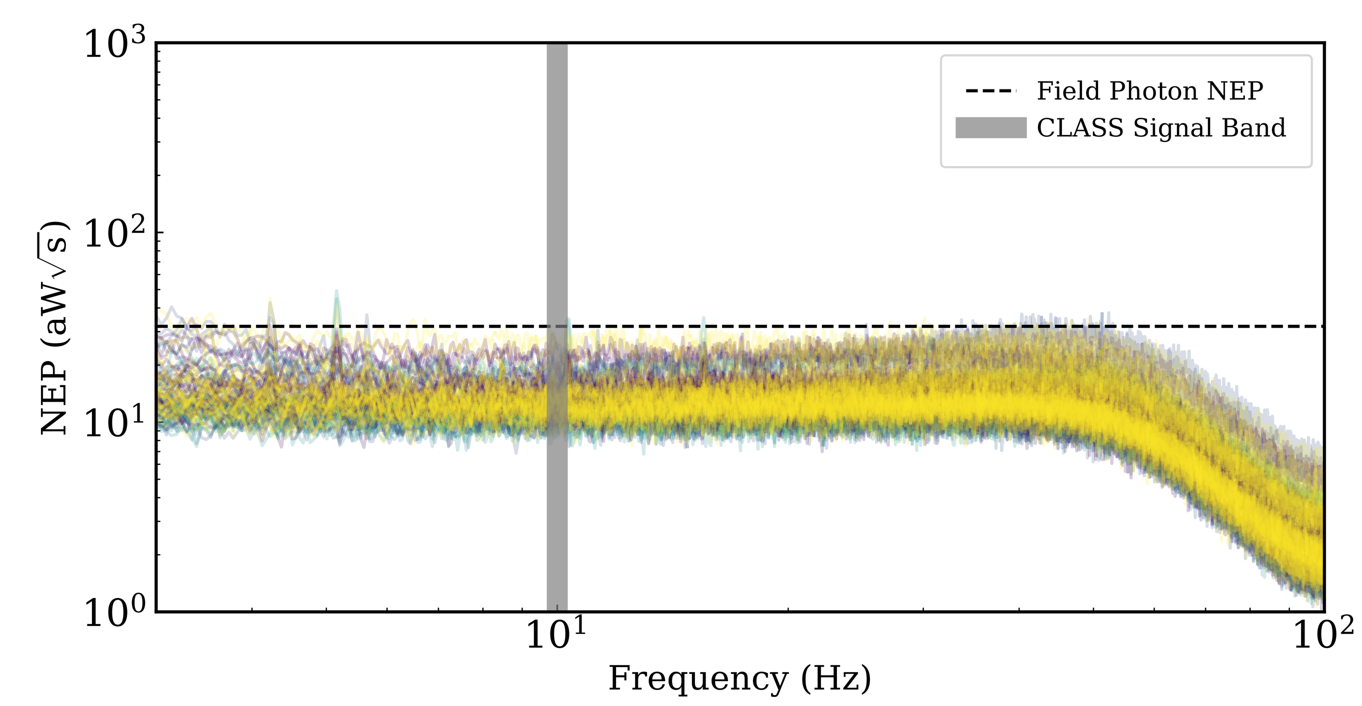

Fig. 8: Measured dark NEP for all four new wafers, with approximately 100 TES bolometers. The grey vertical line shows the modulated CLASS signal band. The dashed horizontal line shows the expected photon NEP at the CLASS site due to the CMB as well as instrumental and atmospheric emission.

The measured detector NEP during dark tests is below the expected NEP of 32 aW$\sqrt{s}$ from photon noise in the field, therefore we expect the new W band detectors to be photon noise limited.

CONCLUSIONS

We present preliminary characterization, via electrothermal parameters, bandpass measurements, and NEP measurements, of four new CLASS 90 GHz detector wafers, which will we will install to upgrade the currently-fielded W1 focal plane. The design includes an updated TES architecture that improves the detector stability and optical efficiency. The new detectors are anticipated to have first light in 2022.

REFERENCES

1. Appel, J. W., Bennett, C. L., Brewer, M. K., et al. 2022, arXiv:2205.06901
2. Chuss, D. T., Ali, A., Amiri, M., et al. 2016, Journal of Low Temperature Physics, 184, 759. doi:10.1007/s10909-015-1368-9
3. Dahal, S., Ali, A., Appel, J. W., et al. 2018, Proc. SPIE, 10708, 107081Y. doi:10.1117/12.2311812
4. Denis, K. L., Cao, N. T., Chuss, D. T., et al. 2009, The Thirteenth International Workshop on Low Temperature Detectors - LTD13, 1185, 371. doi:10.1063/1.3292355
5. Essinger-Hileman, T., Ali, A., Amiri, M., et al. 2014, Proc. SPIE, 9153, 91531I. doi:10.1117/12.2056701
6. Harrington, K., Marriage, T., Ali, A., et al. 2016, Proc. SPIE, 9914, 99141K. doi:10.1117/12.2233125
7. Irwin, K. D., & Hilton, G. C. 2005, Cryogenic Particle Detection, 63.
8. Iuliano, J., Eimer, J., Parker, L., et al. 2018, Proc. SPIE, 10708, 1070828. doi:10.1117/12.2312954
9. Rostem, K., Ali, A., Appel, J. W., et al. 2016, Proc. SPIE, 9914, 99140D. doi:10.1117/12.2234308

Acknowledgements: *We acknowledge the National Science Foundation Division of Astronomical Sciences for their support of CLASS under Grant Numbers 0959349, 1429236, 1636634, 1654494, 2034400, and 2109311. CLASS is located in the Parque Astronómico Atacama in northern Chile under the auspices of the Agencia Nacional de Investigación y Desarrollo (ANID).*